Heat Mass Transfer (2018) 54:553–562
DOI 10.1007/s00231-017-2149-6

ORIGINAL

Numerical simulation of heat transfer in metal foams

Priyatham Gangapatnam[1] · Renju Kurian[1] · S. P. Venkateshan[1]

Received: 1 October 2016 / Accepted: 22 August 2017 / Published online: 13 September 201 7

Abstract This paper reports a numerical study of forced convection heat transfer in high porosity aluminum foams. Numerical modeling is done considering both local thermal equilibrium and non local thermal equilibrium conditions in ANSYS-Fluent. The results of the numerical model were validated with experimental results, where air was forced through aluminum foams in a vertical duct at different heat fluxes and velocities. It is observed that while the LTE model highly under predicts the heat transfer in these foams, LTNE model predicts the Nusselt number accurately. The novelty of this study is that once hydrodynamic experiments are conducted the permeability and porosity values obtained experimentally can be used to numerically simulate heat transfer in metal foams. The simulation of heat transfer in foams is further extended to find the effect of foam thickness on heat transfer in metal foams. The numerical results indicate that though larger foam thicknesses resulted in higher heat transfer coefficient, this effect weakens with thickness and is negligible in thick foams.

Keywords Metal foam · Vertical channel · Porous media · LTE · LTNE · Foam thickness

✉ Renju Kurian
renjukurian@gmail.com

Priyatham Gangapatnam
me10b051@smail.iitm.ac.in

S. P. Venkateshan
01775@retiree.iitm.ac.in

[1] Heat Transfer and Thermal Power Laboratory, Department of Mechanical Engineering, Indian Institute of Technology Madras, Chennai 600036, India

Nomenclature

A	Surface area of the aluminum plate, m^2
a, b	Coefficients of fit in Eq. 15
C	Form drag coefficient, m^{-1}
C_p	Specific heat at constant pressure, J/kg K
h	Heat transfer coefficient, W/m^2 K
K	Permeability of foam assembly, m^2
k_{eff}	Effective thermal conductivity of porous medium defined in Eq. 14, W/m K
k_f	Thermal conductivity of air, W/m K k_s
k_s	Thermal conductivity of solid foam material, W/m K
L	Length of aluminum foam assembly along flow direction, m
Nu_H	Nusselt number based on foam thickness, hH/k_f
PPI	Number of pores per inch of metal foam
ΔP	Pressure drop across test section, Pa
Q	Heat input, W
Q_{loss}	Heat loss through the insulation, W
Re_H	Reynolds number based on foam thickness, UH/ν
T	Surface temperature of aluminum plate, °C
ΔT	Excess temperature of air over ambient defined in Eq. 18, °C
u	Inlet velocity of air in the flow direction, m/s
V	Velocity vector, m/s
E	Total energy of the medium
S	Enthalpy source term

Greek Symbols

μ	Dynamic viscosity of air, kg/m-s
ν	Kinematic viscosity of air, m^2/s
ρ	Density of air, kg/m^3

ϕ	Volumetric porosity of the metal foam

Subscripts

eff	Effective
f	Air
loss	Heat loss through the insulation
s	Solid
∞	Ambient conditions
sf	Solid-fluid interface

1 Introduction

Forced and natural convective heat transfer in porous media has been studied extensively for several decades for their superior heat transfer applications in electronic cooling, geothermal systems and solar collectors. A comprehensive review in this regard is presented in Kaviany [1]. Studies in the past were focused on packed beds and sintered materials for their direct application as naturally occurring porous media. In the past few years, heat transfer in metal foams has been studied extensively as metal foams are reported to have superior thermal performance with a low hydraulic resistance.

Heat transfer in porous medium is generally modeled in two ways. The local thermal equilibrium (LTE) condition assumes identical solid and fluid temperature inside a representative elementary volume (REV) and a single energy equation is used to model heat transfer. The local thermal non equilibrium model (LTNE) relaxes this assumption and utilizes a two equation model. Hunt and Tien [2] studied the effect of thermal dispersion on forced convection in metal foams by considering the simplifying assumption of local thermal equilibrium. Chick et al. [3] obtained an analytical solution for a fully developed forced convection in a gap between two concentric cylinders by considering LTE model. Poulikakos and Renken [4] carried out numerical investigation of forced convection in a channel with fluid saturated porous medium using a single energy equation. Vafai and Kim [5] analyzed forced convection in a channel with porous medium, bounded by two parallel plates. A single equation with the effective thermal conductivity of the porous medium was utilized to analyze the heat transfer. Exact solutions were obtained for velocity and temperature distributions. Hung et al. [6] analyzed the thermal performance of porous-micro channel heat sinks in 3D under the LTE assumption. Amiri and Vafai [7] carried out numerical simulations of forced convective incompressible flow through porous media based on a two equation energy model. They presented the validity of LTE assumption in the form of error maps. Whitaker and Quintard [8] investigated the constraints to be satisfied for the validity of the LTE model. These constraints were validated with numerical experiments for transient heat conduction in two-phase systems. Lee and Vafai [9] investigated the validity of LTE model by obtaining an exact solution for fluid and solid temperatures based on a two equation energy model. It is shown that the heat transfer characteristics in porous media can be classified into three regimes i.e. fluid conduction, solid conduction and an internal heat exchange between the fluid and solid phases. Kim et al. [10] obtained analytical solutions for temperature distributions in a micro channel heat sink using both one-equation and two-equation energy models for heat transfer. They concluded that the LTE assumption becomes valid as the Darcy number decreases, or the effective thermal conductivity increases.

In recent years, a few researchers have utilized the LTNE equation exclusively to model the heat transfer in metal foams and have found that they offer an accurate modeling of heat transfer in metal foams. Phanikumar and Mahajan [11] presented numerical and experimental results of buoyancy induced flows in high porosity metal foams considering the LTNE model and concluded that it provides a superior description of heat transfer in metal foams. Calmidi and Mahajan [12] conducted forced convection heat transfer experiments in high porosity metal foams of porosity in the range 0.89-0.97 with air and water as fluid medium in a horizontal channel. The energy transport is modeled without invoking the LTE assumption. More research on LTNE studies can be found in references Jiang et al. [18] Angirasa [19] and Zhao et al. [20].

Some researchers have investigated the effect of foam thickness on heat transfer in metal foams. Salas and Waas [13] conducted forced convection experiments in aluminum metal foams with air as the working fluid. Four foams of thickness in the range of 6.4 mm to 25.4 mm were utilized for this purpose. They concluded that larger foam thickness resulted in increased heat transfer but this effect diminishes for thicker foams. Mancin et al. [14, 15] conducted heat transfer experiments in a horizontal channel with aluminum foams of 20 and 40mm thickness. The results indicate that foam thickness had no significant effect on heat transfer. Kamath et al. [16] conducted mixed convection heat transfer and hydrodynamic experiments in a vertical channel with aluminum and copper metal foams. They concluded that heat transfer in metal foams is a strong function of foam thickness and it increases with foam thickness.

The review of above literature suggests that even though there have been many studies that consider LTE and LTNE model separately to model heat transfer in metal foams, there are very few studies that compared both models and validated them with experimental results. Further the effect of foam thickness on heat transfer has not been adequately

investigated. The objective of this study is to simulate the heat transfer in metal foams considering both LTE and LTNE conditions using the commercial software ANSYS and validate the results with experiments which have been conducted under identical conditions. Numerical simulations have been further extended to find the effect of foam thickness on heat transfer in metal foams.

2 Numerical simulation

2.1 Physical model and mathematical formulation

A schematic of the computational domain is shown in Fig. 1, along with the orientation of the axes. Air is assumed to enter the metal foam at a uniform velocity as determined experimentally. A known amount of heat flux is given to the heated wall. The temperature gradients are zero for both solid and fluid phases at the adiabatic wall.

2.1.1 Governing equations

The continuity equation assumes a steady and incompressible fluid flow through the metal foam. Standard momentum and energy equations as used in Calmidi and Mahajan [12] are utilized in this numerical study.

Continuity equation:

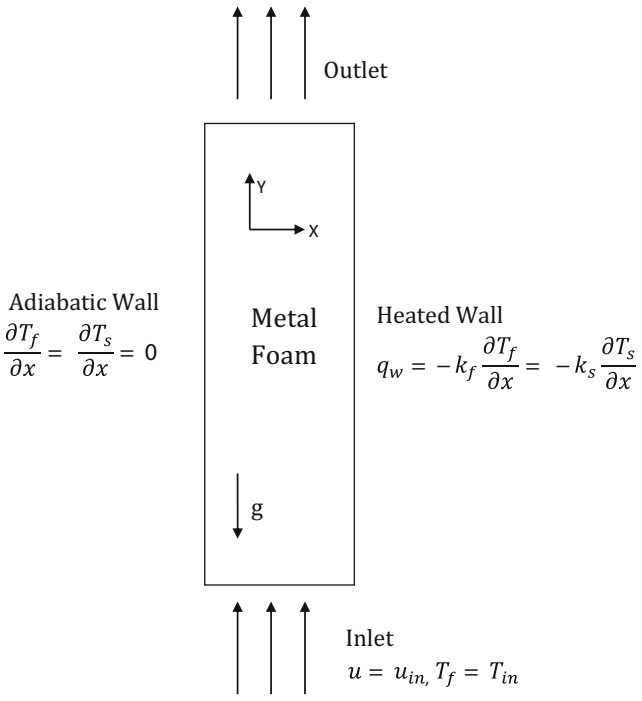

Fig. 1 Schematic of computational domain with boundary conditions

The continuity equation assumes a steady, incompressible fluid flow through the porous medium given by Eq. 1.

$$\frac{\partial u}{\partial y} = 0 \tag{1}$$

Momentum equation:

The steady state momentum equation in the volume averaged form is given by Eq. 2.

$$-\frac{\partial P}{\partial y} + \frac{\mu}{\phi}\frac{\partial^2 u}{\partial x^2} - \frac{\mu}{K}u - \frac{\rho_f}{K}u^2 = 0 \tag{2}$$

where ϕ and K are the porosity and the permeability of the medium respectively. The third and fourth term in the right hand side of Eq. 2 side account for the pressure drop due to viscous friction and form drag respectively.

Energy equations:

LTE Model:

The local thermal equilibrium assumption results in a single energy equation considering the effective thermal conductivity of medium, and is given by Eq. 3.

$$(\rho c_p)_f u.\frac{\partial T}{\partial y} = k_e\left(\frac{\partial^2 T}{\partial y^2} + \frac{\partial^2 T}{\partial x^2}\right) \tag{3}$$

where k_e is the effective thermal conductivity of the metal foam. The effective thermal conductivity in this study is considered as the geometric mean of the conductivities of two phases given by Nield's model as mentioned in the next section.

LTNE Model:

The energy equations of fluid and solid considering the assumption of local thermal non equilibrium are given by Eqs. 4 and 5.

Fluid energy equation:

$$\phi k_f\left(\frac{\partial^2 T_f}{\partial y^2} + \frac{\partial^2 T_f}{\partial x^2}\right) + h_{sf}.a_v.(T_s - T_f) = 0 \tag{4}$$

Solid energy equation:

$$(1-\phi)k_s\left(\frac{\partial^2 T_s}{\partial y^2} + \frac{\partial^2 T_s}{\partial x^2}\right) + h_{sf}.a_v.(T_f - T_s) = 0 \tag{5}$$

h_{sf} and a_v are the interfacial heat transfer coefficient and interfacial area density respectively.

2.1.2 Boundary conditions

Inlet:

$$u = u_{in}, T_f = T_{in}; \tag{6}$$

Adiabatic wall:

$$q_w = 0, \frac{\partial T_f}{\partial x} = \frac{\partial T_s}{\partial x} = 0 \tag{7}$$

Heated wall:

$$q = q_w = -k_f \frac{\partial T_f}{\partial x} = -k_s \frac{\partial T_s}{\partial x} \tag{8}$$

Outlet:

$$\frac{\partial T_f}{\partial y} = \frac{\partial T_s}{\partial y} = 0 \tag{9}$$

2.2 Numerical simulation in ANSYS-Fluent

Finite Volume based software ANSYS-Fluent 14.5 is used to simulate the fluid flow and heat transfer in the porous media. This software is having inbuilt module for porous media simulations. A 2D geometry of the aluminum foam was created using the design modeler in FLUENT. The geometry in this case is a two dimensional rectangular duct having dimensions 150 mm × 10 mm. The fluid flows in the Y direction along a length of 150 mm. The duct is filled with the metal foam of the same external dimensions.

Grid Sensitivity Study:

Meshing is done in the geometry to discretize the domain into large number of cells or control volumes. The geometry is divided into a large number of cells based on the size of each cell, which can be specified in the sizing option in FLUENT. A mesh dependence study is carried out to select the optimum number of cells to save the computational effort without compromising on the accuracy. The element size is chosen when the average heated wall temperature does not vary more than 0.1 °C. Table 1 presents the results of grid sensitivity study carried out.

Figure 2 shows the variation of average surface temperature of heated wall with the number of cells used in the grid sensitivity study.

In LTNE modeling, FLUENT utilizes a dual cell approach. A solid zone, which is spatially coincident with the fluid zone is created, and both the zones are solved simultaneously and are coupled only through heat transfer.

Table 1 Grid sensitivity study

Cell size	Number of cells	Average heated wall temperature, K
0.001	1500	314.56
0.0008	2344	314.06
0.0006	4167	313.77
0.0005	6000	313.58
0.0004	9375	313.45
0.0003	16667	313.38
0.00025	24000	313.33
0.0002	37500	313.30

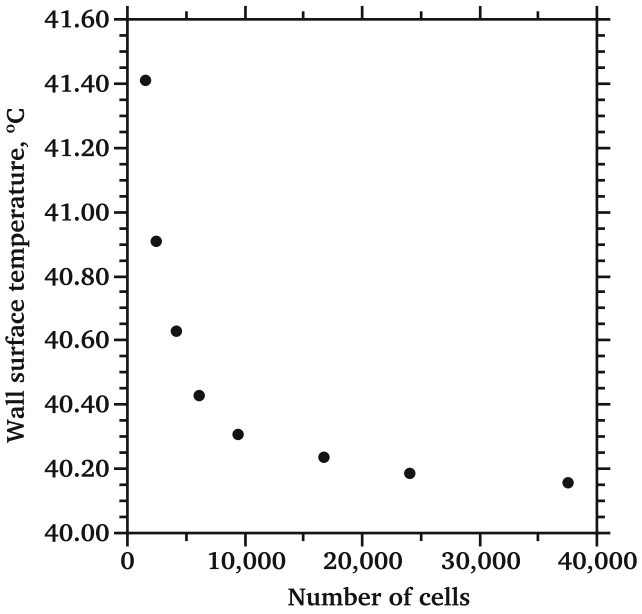

Fig. 2 Variation of heated wall temperature with number of cells

2.2.1 Mathematical formulation in ANSYS-fluent

Momentum Equations:

FLUENT by default uses the Superficial Velocity Porous Formulation to model single phase flow in porous media. The superficial velocity is calculated based on the volumetric flow rate in the computational domain. In FLUENT, an additional source term is added to the standard flow equations to model fluid flow in porous media. The source term accounts for both the viscous loss and inertia loss. Equation 10 is the algebraic momentum equation used in FLUENT at each node.

$$S_i = -\sum_{j=1}^{3} D_{ij}\mu v_j + \sum_{j=1}^{3} C_{ij}\frac{1}{2}\rho|v|v_j \tag{10}$$

For a simple case of a homogeneous medium, the equation is given below.

$$S_i = -\left(\frac{\mu}{K}v_i + C\frac{1}{2}\rho|v|v_i\right) \tag{11}$$

This equation is the same as the Hazen-Darcy-Dupuit equation and hence the experimentally determined permeability and form drag coefficients are adopted here.

Energy equations in ANSYS-Fluent (http://users.ugent.be/~mvbelleg/flug-12-0.pdf):

LTNE Modeling:

Energy equations in the LTNE modeling are considered without the assumption of local thermal equilibrium. The dual cell approach is used here. The energy equations are solved separately for the fluid and solid zones. Interfacial

heat transfer coefficient is an important parameter that is required to obtain a closure in solid and fluid state energy equations. The fluid to solid heat transfer coefficient was taken from Wakao et al. [22] and is given by Eq. 12.

$$h_{sf} = \frac{k_f}{d_p}[2 + 1.1 Pr^{\frac{1}{3}} Re_d^{0.6}] \quad (12)$$

Interfacial area density and heat transfer coefficient need to be entered manually in FLUENT to solve these equations. In FLUENT, the interfacial area density is defined as the area of solid in contact with the fluid per unit volume. It is calculated considering the porosity, pore diameter and fiber diameter. The model adopted for calculating the interfacial area density is that of the arrays of parallel cylinders intersecting at three mutual perpendicular directions given by Eq. 13.

$$a_{sf} = \frac{3(\pi)d_f}{d_p^2} \quad (13)$$

LTE Modeling:

The LTE model in FLUENT uses the effective thermal conductivities of the solid and fluid medium, which in this case is calculated by the Nield's model [21] of effective thermal conductivity, and is given by Eq. 14.

$$k_e = k_f^{\phi}.k_s^{1-\phi} \quad (14)$$

It should be noted that FLUENT uses an effective thermal conductivity considering the arithmetic average of fluid and solid conductivities. The solid conductivity is adjusted to get the effective thermal conductivity as given by Nield's model. The thermal properties of air are evaluated at the mean value of inlet and exit temperatures.

Assumptions in the FLUENT modeling:

1) The metal foam is assumed to be homogeneous and isotropic.
2) The flow in this study is assumed to be in steady state and incompressible.
3) The working fluid is air with constant thermo-physical properties calculated at the mean temperature of inlet and outlet.
4) Flow and heat transfer simulations are performed in the laminar regime with Reynolds numbers in the range of 11.73 to 1903. The reason behind this assumption is that air flow is very much ordered through the pores.
5) Thermal dispersion is assumed to be negligible and is not considered in the simulation. Calmidi and Mahajan [12] conducted experiments in high porosity aluminum foams with air as the fluid medium, and concluded that for metal foam and air combinations, where the thermal conductivity of solid matrix is high, the effects of thermal dispersion are negligible.

The hydrodynamic parameters to be used in the software are obtained from experiments, the details of which are discussed in the next section.

3 Experimental setup and procedure

Figures 3 and 4 show the photographs of the experimental setup and schematic of the test section respectively. The setup consists of a test section mounted on a vertical wind tunnel. The test section includes a heater plate assembly placed at the center, bounded by the metal foams on either side. The wind tunnel has an axial fan at the bottom to blow air. The arrangement resembles a vertical channel of size 150 mm×250 mm×10 mm filled with metal foam. A bell mouth is provided at the entry to minimize the entry losses. Five K-type thermocouples (32-AWG) are fixed on each side of the aluminum plate using copper cement. The thermocouples have a maximum measurement error of ±0.1 °C and are calibrated using a constant temperature bath (Make: Julabo, Model: FP50). The thermocouples are connected to a PC based data acquisition system (Make: Agilent, Model: 34 970A). A DC power source (Make: Aplab), which has a range of 30-600V and 0-1.5 A, supplies power input to the heater. A thermal anemometer (make TESTO, model:

Fig. 3 Experimental setup

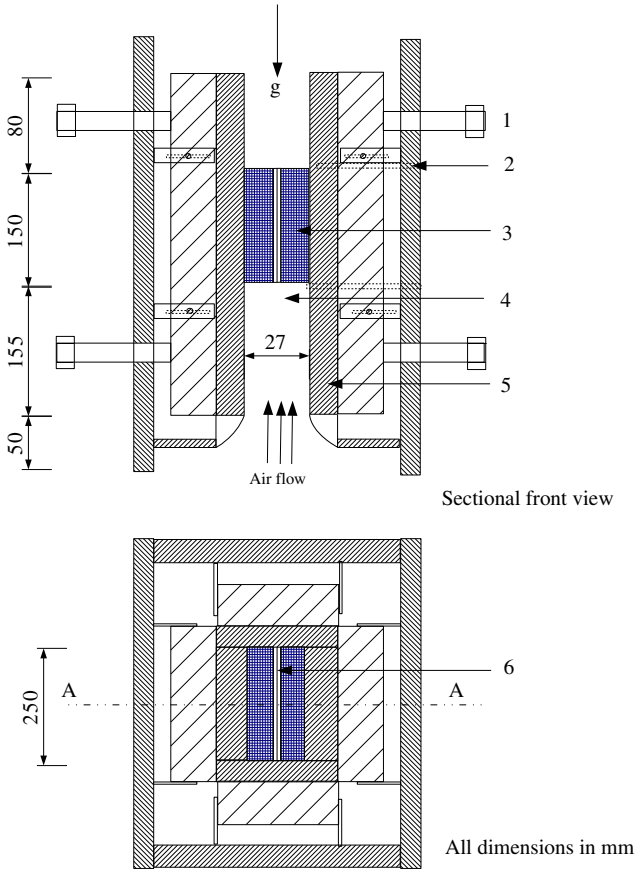

1. Tightening screws 2. Pressure tap 3. Mesh foam 4. Vertical duct 5. Non-rubberized cork 6. Mica heater

Fig. 4 Schematic of the test section

425) is utilized to measure the temperature and velocity at the inlet section. The velocity is measured at ten different positions at the same level and the average value is taken as the inlet velocity. The air velocity is varied by varying the speed of the axial flow fan mounted below the wind tunnel. A digital differential pressure transducer (Make: TESTO, Model: 512) with 0.1 Pa resolution, connected to pressure taps located across the test sample is used to measure the pressure drop across the metal foam. The heater plate is given different heat fluxes by varying the voltage levels in the D C power source. The heat loss across the cork sheet is also accounted for by measuring the temperature drop across the sheet using K-type thermocouple, four on each side.

The experiments are conducted for three power inputs to the heater (20, 40 and 60 W) and inlet flow velocities ranging from 0 to 1.52 m/s. Scanning Electron Microscope (SEM) analysis is conducted on the metal foam to determine the material composition, and is found similar to that of AlSi7Mg. Based on this, the thermal conductivity of the aluminum foam is taken as 165 W/mK. The procedure is detailed in Kamath et al. [16]. Table 2 lists the characteristics of the metal foams used in the study. The volumetric porosity of the foams is determined, by measuring the dry mass of the metal foam and dividing it by density to get the solid volume. The pore diameter and fiber diameter are important to calculate the interfacial heat transfer coefficient and specific surface area. A complete characterization of the metal foams is elaborated in Kamath et al. [16]. Table 3 lists the thermo-physical properties of the fluid and solid phases used in the experiments.

4 Results and discussion

4.1 Hydrodynamic experiments

Hydrodynamic experiments are essential in this study to determine the permeability and form drag coefficient which are input parameters in FLUENT. Pressure drop measurements across the metal foam are done at different velocities and are plotted to fit a second degree polynomial as given by Eq. 15. The equation is compared with Hazen-Darcy-Dupuit (Eq. 16), to obtain the permeability and form drag coefficient. Figure 5 shows the variation of pressure drop with fluid inlet velocity.

The permeability (K) and form drag coefficient (C) of the metal foam used in this study are determined to be 3.34 x 10^{-7} m^2 and 232.27 m^{-1} respectively(see Eq. 16).

$$\frac{\Delta P}{L} = aU + bU^2 \tag{15}$$

$$\frac{\Delta P}{L} = \frac{\mu}{K}U + \rho C U^2 \tag{16}$$

4.2 Heat transfer experiments

The average surface temperature of the aluminum plate is used to determine the heat transfer coefficient. The heat transfer coefficient is determined by Eq. 17 based on temperature excess i.e. the difference between the wall temperature and the ambient temperature.

$$h = \frac{Q - Q_{loss}}{2A\Delta T} \tag{17}$$

where the average wall temperature ΔT is defined by Eq. 18.

$$\Delta T = \frac{1}{n}\sum_{i=1}^{n}(T_i) - T_\infty \tag{18}$$

where Q is the heat input to the heater obtained as the product of voltage and current supplied by the DC power supply. Q_{loss} is the heat loss through cork estimated by a simple conduction analysis along the layers of the cork insulation. The factor '2' is to take into account the heat transfer from

Table 2 Metal foam characteristics

Material	PPI	L×W×H (mm)	Pore diameter (mm)	Fiber diameter (mm)	Porosity (ϕ)
Aluminum	20	250×150×10	3.416	0.451	0.92

both sides of the aluminum plate. The Reynolds number and the Nusselt number used in the present study are defined by Eqs. 19 and 20 respectively.

$$Nu_H = \frac{hH}{k_f} \tag{19}$$

$$Re_H = \frac{uH}{\nu} \tag{20}$$

Considering the results of numerical simulations, the average heated wall temperature is used to compute the heat transfer coefficient and Nusselt number. These are validated with the experimental results. Figure 6 presents the Nusselt number variation with Reynolds number for LTE modeling, LTNE modeling and experiments for the case of 10 mm thickness and 20 W heat input at velocities ranging from 0.02 m/s to 1.52 m/s. It is observed that LTE model under predicts the Nusselt number by 30-50%. This deviation increases with Reynolds number. At the highest Reynolds number of 325, the experimental Nusselt number is 21.65, whereas the LTE model predicts a Nusselt number of 12.25, a deviation of 43%. The underlying assumption in LTE modeling is that the temperatures of fluid and solid inside a REV are same, which is the main reason for the deviation between predicted and experimental values.

One of the criteria for the LTE assumption to be valid is that the properties of fluid and solid have to be similar [24]. This enables the fluid to bring the temperature of the solid phase to its temperature making the LTE condition valid. In cases where the thermal conductivities of fluid and solid differ substantially, this assumption stands invalid. In the present study the thermal conductivity of aluminum is 164 W/mK while the thermal conductivity of air at 30 °C is 0.0264 W/mK, which is very much less compared to the solid thermal conductivity.

Another favorable condition for the LTE model is at lower Reynolds number [23]. A lower Reynolds number indicates that the fluid flow rate is less. This enables the fluid to have enough time to exchange heat with the solid. A higher Reynolds number indicates higher flow rate of the fluid making the fluid less capable of exchanging heat with the solid. As the velocity increases the solid and fluid temperature difference inside the REV further increases and is reflected in the increasing deviation at higher velocities. Hence the LTNE model, which does not assume the conditions of thermal equilibrium between the two phases, is considered for further analysis.

Figure 7 presents the Nusselt number variation with Reynolds number in the velocity range of 0.02 m/s to 1.52 m/s, using the LTNE model.

The model predicts accurately the Nusselt number within 2-15% of the experimental value. It is also observed that the Nusselt number varies very little with different fluxes and the same is being predicted by the LTNE Model. The heat transfer coefficient when the inlet air velocity is 1.52 m/s at 20 W heat flux is 57 W/m^{2}K and the LTNE model predicts a value of 56.95 W/m^{2}K. Figure 8 compares the fluid temperature contours as predicted by the LTNE model at three different velocities. As the velocity increases, the heat transfer coefficient between the fluid and solid matrices increases resulting in increased heat transfer and decreased fluid temperature for the same heat flux.

An important observation in this study is that, at higher Reynolds number the LTNE simulation under predicts the experimental results by 10-15%. The same observation was noted by Calmidi and Mahajan [12]. This deviation is attributed to turbulence and this phenomenon is not considered in the simulation in FLUENT.

Few researchers have investigated experimentally the Reynolds number at which the flow becomes turbulent. Horton and Pokrajac [25] conducted experiments on turbulent flows through a regular porous matrix of spheres packed in a cubic arrangement.The pore Reynolds number of the experiments ranged between 70 and 430. They identified three different regimes: unsteady laminar, transition to turbulence and turbulent. It is mentioned that the onset of turbulence started at a pore Reynolds number of 170. In the present

Table 3 Thermo-physical properties of the solid and fluid

Phase	Material	Thermal Conductivity (W/mK)	Specific Heat Capacity (J/kgK)	Density (kg/m^3)
Solid	Aluminum	165	900	2700
Fluid	Air (@ 30°)	0.02675	1005	1.165

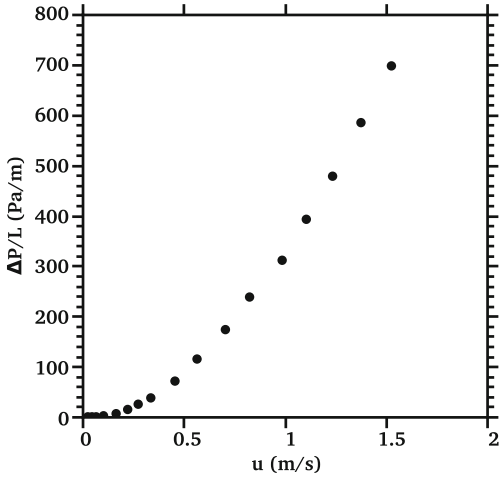

Fig. 5 Variation of pressure drop per unit length with fluid inlet velocity

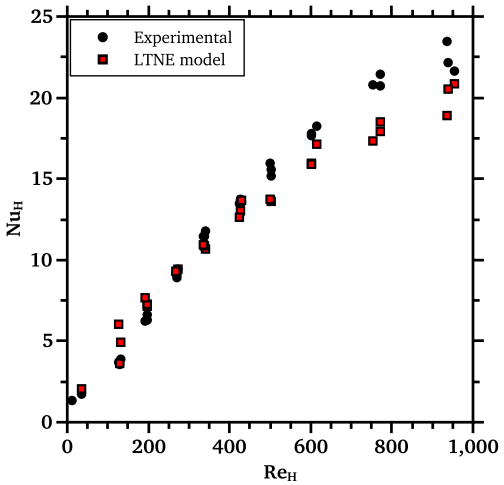

Fig. 7 Variation of Nusselt number with Reynolds number for different heat fluxes

study, considering the pore diameter, the pore Reynolds number range from 5 to 345. The pore Reynolds number of 170 corresponds to a Reynolds number of 500 (based on thickness) and and this can be the value at which the flow starts to become turbulent. Hence, a slight deviation in the values of simulated Nusselt number and the experimental Nusselt number can be expected at Reynolds numbers above 500. The effect of thermal dispersion can be assumed to be negligible, as indicated by Calmidi and Mahajan [12].

The experimental and LTNE simulation results of the present study are compared with the experimental results of Kamath et al. [16]. They conducted experiments using high porosity aluminum and copper foams of porosities ranging from 0.86 to 0.92 to investigate the effect of foam thickness on heat transfer. They used foams of thickness of 10, 20 and 30 mm thickness. The results of 10 mm thickness aluminum foam are used for comparison. It is to be noted that Nusselt number and Reynolds number expression used in Kamath et al. [16] differ by a factor of 2, as they considered total thickness as two times the foam thickness. Hence, the results in Kamath et al. [16] are reduced by a factor of 2 and compared with the current results. Figure 9 presents the comparison of Nusselt number from experimental study, numerical simulation and Kamath et al. [16]. Both the experimental and simulated results are close to the Nusselt number values as reported by Kamath et al. [16]. The Nusselt number as reported by them for a Reynolds number of 952 is 24.5, while the present LTNE model predicts a Nusselt number of 21, a deviation of 8%. This deviation may be due to the

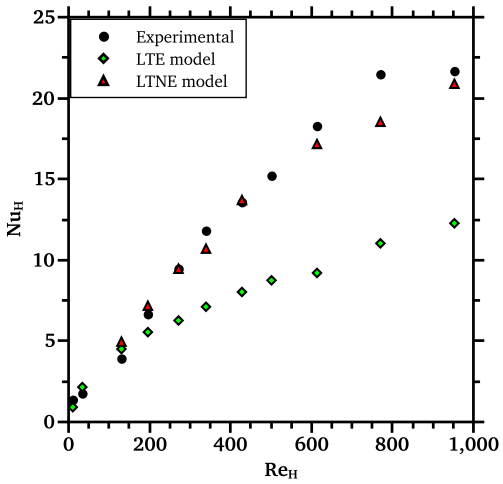

Fig. 6 Variation of Nusselt number with Reynolds number considering both LTE and LTNE models

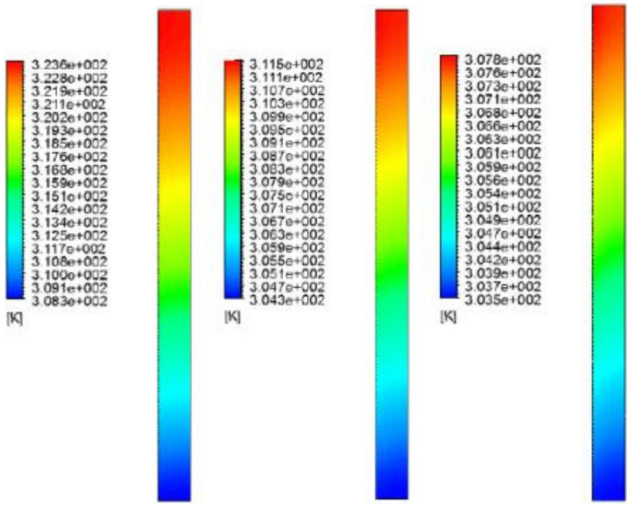

a) Fluid Temperature Contour: u = 0.33 m/s, Q = 40W

b) Fluid Temperature Contour: u = 0.7 m/s, Q = 40W

c) Fluid Temperature Contour: u = 1.52 m/s, Q = 40W

Fig. 8 Fluid temperature contours at different velocities

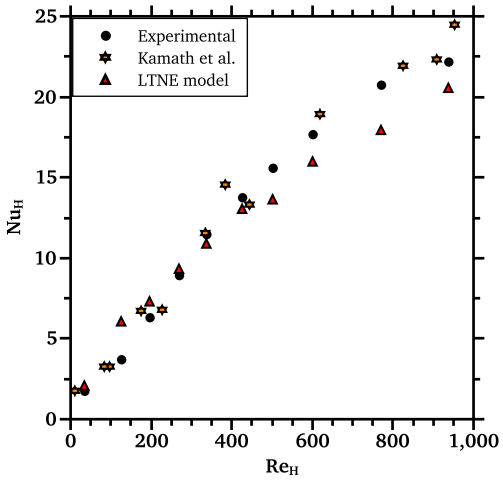

Fig. 9 Comparison of Nusselt number variation with similar porous media

difference in the porosity, permeability, pore diameter and fiber diameter of the foams used in the respective studies.

4.3 Effect of foam thickness on heat transfer

The numerical simulations were extended to identify the effect of foam thickness on heat transfer. Foams used in the present simulations have the same characteristics as that of the earlier simulations, but with a thickness of 5, 20 and 30 mm. A constant inlet temperature of 30 °C and a heat input of 40 W are considered for the simulation. The velocity range also remains the same as in the previous simulations.

Figure 10 presents the variation of heat transfer coefficient with inlet velocity for four different foam thicknesses i.e. 5, 10, 15 and 20 mm. It is observed that the heat transfer coefficient increases with increase in foam thickness. However, it was noticed that this effect reduces with thickness. An increase of foam thickness from 5 mm to 10 mm with an air inlet velocity of 1.52 m/s resulted in a heat transfer coefficient increment by 42%. However, increasing the thickness form 10 mm to 20 mm and 20 mm to 30 mm resulted only in a 12% and 5.35% increase in heat transfer coefficient respectively. A similar observation was reported by Salas and Waas [13] in their study. The authors investigated experimentally the effect of foam thickness on convective heat transfer coefficient and modeled the heat transfer using a finite element approach.

Considering the above data points, a correlation for Nusselt number in terms of aspect ratio (L/H)and Reynolds number is developed, as shown below.

$$Nu_H = 1.66 {Re_H}^{0.63} (L/H)^{-0.67} \tag{21}$$

This correlation is valid for aluminum metal foams in the following range of parameters:

$$11.71 < Re < 1903 \tag{22}$$

$$5 < L/H < 30 \tag{23}$$

The correlated Nusselt number is plotted along with the simulated Nusselt number in Fig. 11. A deviation within ±15% is found between the correlated data and the simulated data. The correlation is valid for foams of porosity close to 0.92. The correlation has been developed with 53 number of numerical data points, and has an R^2 value of 0.96, with a standard error of 3.204.

4.4 Uncertainty analysis

The uncertainties in the measured primary physical quantities are shown in Table 4. The propagation of error due to the

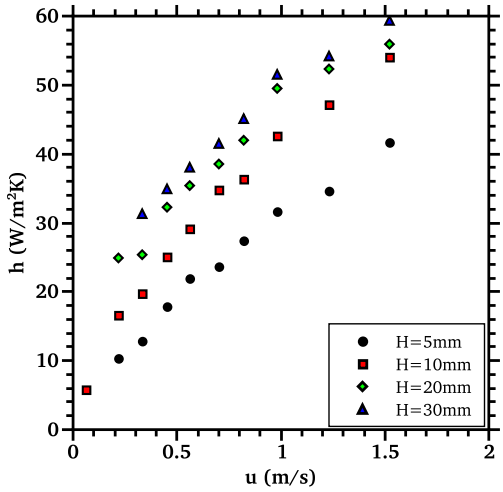

Fig. 10 Variation of heat transfer coefficient with inlet velocity for foams of different thickness

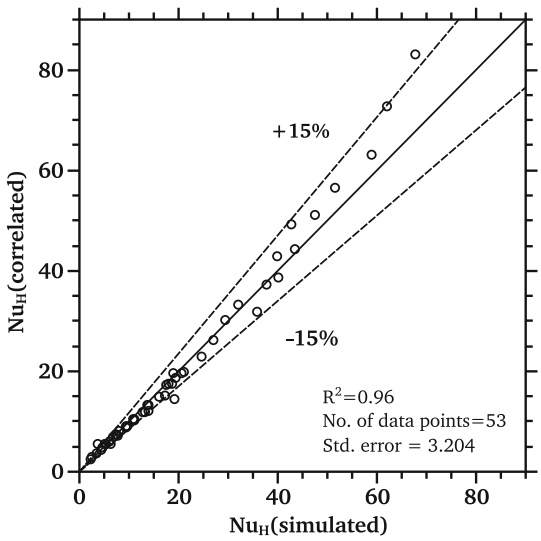

Fig. 11 Parity plot showing comparison of correlated and experimental values of Nusselt number

Table 4 Maximum uncertainty in the measured quantities

Sl. No	Quantity	Uncertainty
1	Temperature	± 0.1 °C
2	Pressure drop	± 0.1 Pa
3	Velocity	± 0.01 m/s
4	Voltage	± 1 V
5	Current	± 0.01 A
6	Heat input	±4.6%
7	Heat transfer coefficient	± 7.5%
8	Nusselt number	± 7.5%
9	Reynolds number	± 8.3%

uncertainties in the measured primary physical quantities into derived quantities are calculated using the procedure described in Venkateshan [17].

$$\sigma_s = \pm \left(\sum_{i=1}^{n} \left[\left(\frac{\partial S}{\partial x_i} \right)^2 \sigma_{x_i}^2 \right] \right)^{\frac{1}{2}} \tag{24}$$

5 Conclusions

Forced convection heat transfer characteristics in high porosity aluminum metal foams were numerically simulated using LTE and LTNE assumptions. The permeability and form drag coefficient values obtained from hydrodynamic experiments were used in ANSYS-Fluent to simulate LTE and LTNE models. The results were further verified with experiments conducted under identical conditions. It was observed that LTE model could predict the Nusslet number correctly for Reynolds number up to 200, beyond which the model under predicts. It has been identified that the high solid to fluid thermal conductivity ratio and lesser time for heat exchange between the phases with increasing Reynolds number, as the probable reasons for the deviation. The results of the LTNE model were found to be in good agreement with experimental results and were within 15 percent of the experimental values. This deviation occurred at higher Reynolds number, which is attributed to the onset of turbulence. The numerical simulations were further extended to study the effect of foam thickness on heat transfer. The results indicated that though heat transfer increases with thickness, this effect reduces at higher foam thicknesses. A correlation for Nusselt number has been developed using the LTNE model.

References

1. Kaviany M (1991) Principles of heat transfer in porous media. Springer-Verlag, New York
2. Hunt M, Tien C (1988) Effects of thermal dispersion on forced convection in fibrous media. Int J Heat Mass Transfer 31(2):301–309
3. Chikh S, Boumedien A, Bouhadef K (1995) Analytical solution of non-Darcian forced convection in an annular duct partially filled with a porous medium. Int J Heat Mass Transfer 38(9):1543–1551
4. Poulikakos D, Renken K (1987) Forced convection in a channel filled with porous medium, including the effects of flow inertia, variable porosity, and Brinkman friction. ASME J Heat Transfer 109:880–888
5. Vafai K, Kim SJ (1989) Forced convection in a channel filled with a porous medium: an exact solution. ASME J Heat Transfer 111:1103–1106
6. Hung T C, Huang YX, Yan WM (2013) Thermal performance analysis of porous-micro channel heat sinks with different configuration designs. Int J Heat Mass Transfer 66:235–243
7. Amiri A, Vafai K (1994) Analysis of dispersion effects and non-thermal equilibrium, non-Darcian, variable porosity, incompressible flow through porous media. Int J Heat Mass Transfer 37:939–954
8. Quintard M, Whitaker S (1995) Local thermal equilibrium for transient heat conduction: theory and comparison with numerical experiments. Int J Heat Mass Transfer 38:2779–2796
9. Lee DY, Vafai K (1999) Analytical characterization and conceptual assessment of solid and fluid temperature differentials in porous media. Int J Heat Mass Transfer 42:423–435
10. Kim SJ, Kim D, Lee DY (2000) On the local thermal equilibrium in micro channel heat sinks. Int J Heat Mass Transfer 43:1735–1748
11. Phanikumar MS, Mahajan RL (2002) Non-Darcy natural convection in high porosity metal foams. Int J Heat Mass Transf 45:3781–3793
12. Calmidi V, Mahajan R (2000) Forced convection in high porosity metal foams. ASME J Heat Transf 122:557–565
13. Salas K, Waas A (2007) Convective heat transfer in open cell metal foams. ASME J Heat Transf 129:1217–1229
14. Mancin S, Zilio C, Rossetto L, Cavallini A (2011) Foam height effects on heat transfer performance of 20 ppi aluminum foams. Appl Therm Eng 1–6
15. Mancin S, Zilio C, Rossetto L, Cavallini A (2011) Heat transfer performance of aluminum foams. ASME J Heat Transfer 133:060904-060909
16. Kamath PM, Balaji C, Venkateshan SP (2013) Convection heat transfer from aluminium and copper foams in a vertical channel. An experimental study. Int J Therm Sci 64:1–10
17. Venkateshan SP (2015) Mechanical measurements. Ane Books, New Delhi
18. Jiang PX, Ren ZP (2001) Numerical investigation of forced convective heat transfer in porous media using a thermal non-equilibrium model. Int J Heat Fluid Flow 22:102–110
19. Angirasa D (2002) Forced convective heat transfer in metallic fibrous materials. Int J Heat Mass Transfer 124:739–745
20. Zhao CY, Lu TJ, Hodson HP (2006) Natural convection in metal foams with open cells. Int J Heat Mass Transfer 48:2452–2463
21. Nield DA, Bejan A (2000) Convection in porous media, 2nd edn. Springer, New York
22. Wakao N, Kaguei S, Funazkri T (1979) Effect of fluid dispersion coefficients on particle-to-fluid heat transfer co-efficients in packed beds. Chem Eng Sci 34:325–336
23. Khashan SA, Al-Nimr MA (2005) Validation of the local thermal equilibrium assumption in forced convection of non-Newtonian fluids through porous channels. Transp Porous Media 61:291–305
24. Whitaker S (1999) The method of volume averaging, theory and applications of transport in porous media, Dorderecht: Kluwer Academic, 13:89
25. Horton N, Pokrajac D (2009) Onset of turbulence in a regular porous medium: an experimental study. Phys Fluids, 21(4), Article number 045104